

**SrSi<sub>6</sub>N<sub>8</sub>—A Reduced Nitridosilicate with a Si–Si Bond\*\***

*Florian Stadler, Oliver Oeckler, Jürgen Senker,  
Henning A. Höppe, Peter Kroll, and Wolfgang Schnick\**

*Dedicated to Professor Arndt Simon  
on the occasion of his 65th birthday*

Silicates are a very important class of minerals that form about 80 wt% of the earth's crust. Nearly all naturally occurring silicates are oxosilicates. However, sinoite (Si<sub>2</sub>N<sub>2</sub>O), a mineral that occurs in meteorites, contains a framework of corner-sharing Si(O,N)<sub>4</sub> tetrahedrons.<sup>[1,2]</sup> In the

---

[\*] Dipl.-Chem. F. Stadler, Dr. O. Oeckler, Dr. J. Senker,  
Prof. Dr. W. Schnick  
Department Chemie und Biochemie  
Ludwig-Maximilians-Universität  
Lehrstuhl für Anorganische Festkörperchemie  
Butenandtstrasse 5–13(D), 81377 München (Germany)  
Fax: (+49) 89-2180-77440  
E-mail: wolfgang.schnick@uni-muenchen.de

Dr. H. A. Höppe  
New address: Institut für Anorganische Chemie  
Albert-Ludwigs-Universität  
Albertstrasse 21, 79104 Freiburg (Germany)

Dr. P. Kroll  
Institut für Anorganische Chemie  
RWTH Aachen  
Professor-Pirlet-Strasse 1, 52056 Aachen (Germany)

[\*\*] This work was supported by the Fonds der Chemischen Industrie and the Deutsche Forschungsgemeinschaft.

past few years an increasing number of nitridosilicates has been synthesized. The characteristic structural entities in oxo- and nitridosilicates as well as in oxonitridosilicates (sions) are  $\text{SiX}_4$  tetrahedrons ( $\text{X} = \text{O}, \text{N}$ ), which are typically connected through common corners ( $\text{X} = \text{O}, \text{N}$ )<sup>[3a]</sup> or edges ( $\text{X} = \text{N}$ ).<sup>[3b]</sup> Higher coordination numbers of silicon ( $\text{CN} > 4$ ) mainly occur in high-pressure phases (e.g. the  $\text{SiO}_2$  polymorph stishovite or perovskite-type  $(\text{Mg}, \text{Fe})\text{SiO}_3$ ).<sup>[4]</sup>

All known crystalline silicates exhibit Si–X substructures, in which Si and X atoms ( $\text{X} = \text{O}, \text{N}$ ) alternate in a strictly regular fashion. According to IUPAC nomenclature, the term “silicate” indicates a compound with silicon in the oxidation state +IV. Very few reduced silicon oxides and nitrides have been reported that contain silicon in oxidation states  $< +\text{IV}$ . For example, Hengge synthesized an amorphous subnitride with the postulated formula  $\text{Si}_6\text{N}_2$  starting from  $\text{CaSi}_2$  and  $\text{NH}_4\text{Br}$  at  $550^\circ\text{C}$ . He assumed that this compound contained Si–Si bonds (230 pm) although no comprehensive structural model could be ascertained.<sup>[10]</sup> Based on this work Kniep et al. described another subnitride with the formula  $\text{Si}_2\text{N}$ . It was obtained as an amorphous product, too, by the topochemical reaction of  $\text{CaSi}_2$  with  $\text{NH}_4\text{X}$  ( $\text{X} = \text{F}, \text{Cl}, \text{Br}, \text{I}$ ) at  $330\text{--}370^\circ\text{C}$ .<sup>[11]</sup> A structural model with sphalerite- or wurtzite-analogous layers was proposed and a Si–Si distance of 230 pm was assumed, which has not yet been proven by experimental methods. Furthermore, Jansen et al. reported on the amorphous suboxide  $\text{Si}_2\text{O}_3$ .<sup>[12]</sup> The product was obtained by a sol-gel process from  $\text{Si}_2\text{Cl}_6$  and  $\text{H}_2\text{O}$  at  $-75^\circ\text{C}$ . A Si–Si bond length of 230 pm was derived from pair correlation functions.

In the past couple of years we have been focussing on the preparation and characterization of new nitrido- and oxonitridosilicates as well as oxonitridoaluminosilicates (sialons).<sup>[13]</sup> We have now obtained the first crystalline reduced nitridosilicate  $\text{SrSi}_6\text{N}_8$  by reaction of strontium with silicon diimide at  $1630^\circ\text{C}$  in a radio-frequency furnace (see Experimental Section).

The structure of  $\text{SrSi}_6\text{N}_8$  was determined by a single-crystal X-ray structure analysis.<sup>[14]</sup> Considering the stoichiometric formula of the colorless compound, the charge balance does not allow us to assume the presence of exclusively tetravalent silicon. Actually,  $\text{SiN}_4$  tetrahedrons as well as  $\text{N}_3\text{Si–SiN}_3$  entities, in which each nitrogen atom bridges three silicon atoms, occur in  $\text{SrSi}_6\text{N}_8$  (Figure 1, left). Such  $\text{N}^{3-}$

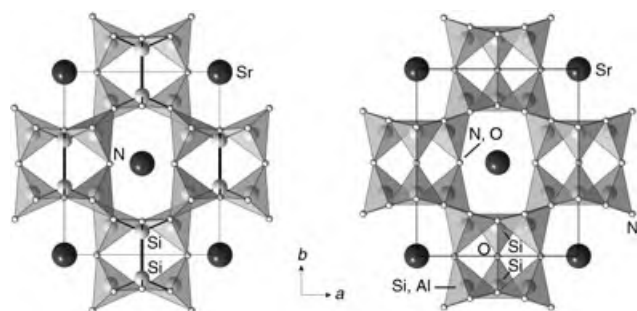


**Figure 1.** Left: Crystal structure of  $\text{SrSi}_6\text{N}_8$  (view along  $[001]$ ). In addition to  $\text{SiN}_4$  tetrahedrons there are  $\text{N}_3\text{Si–SiN}_3$  units with formally trivalent silicon. Right: Crystal structure of  $\text{Sr}_2\text{Al}_x\text{Si}_{12-x}\text{N}_{16-x}\text{O}_{2+x}$  ( $x \approx 2$ )<sup>[16]</sup> (view along  $[001]$ ).

connections are frequently observed in the class of nitrido-silicates.<sup>[3b]</sup> The Si–N bond lengths (166–176 pm) correspond well with those in other nitridosilicates.<sup>[13]</sup> The framework structure of  $\text{SrSi}_6\text{N}_8$  significantly differs from any other known silicate structure as it does not comprise a strictly alternating sequence of Si and X atoms ( $\text{X} = \text{O}, \text{N}$ ). In contrast, it contains additional Si–Si single bonds (235.2(2) pm), the length of which precisely matches (within less than 0.1 %) that of the archetypical covalent Si–Si single bond in diamond-type silicon. It also resembles Si–Si bond lengths of the molecular compounds  $\text{Si}_2\text{H}_6$ ,  $\text{Si}_2\text{F}_6$ , or  $\text{Si}_2\text{Me}_6$ , which range between 213 and 234 pm.<sup>[15]</sup>

The  $\text{Sr}^{2+}$  ions in  $\text{SrSi}_6\text{N}_8$  are ten-coordinate, surrounded by nitrogen at distances of 269–316 pm. A quite similar crystal structure occurs in the sialon  $\text{Sr}_2\text{Al}_x\text{Si}_{12-x}\text{N}_{16-x}\text{O}_{2+x}$  ( $x \approx 2$ ; Figure 1, right), which also crystallizes in the space group  $\text{Imm}2$ .<sup>[16]</sup> Comparing the tetrahedron frameworks of the two structures (Figure 2), it is evident that in the sialon an oxygen

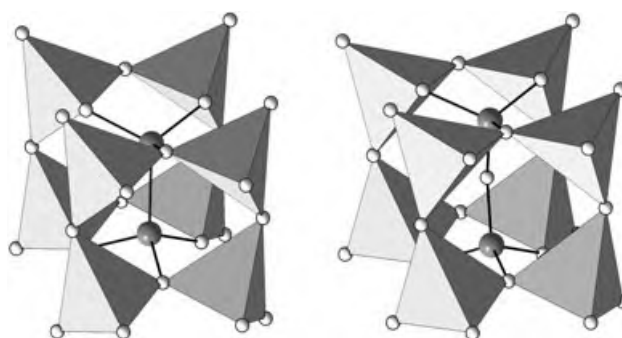


**Figure 2.** Tetrahedron frameworks in  $\text{SrSi}_6\text{N}_8$  (left) and in  $\text{Sr}_2\text{Al}_x\text{Si}_{12-x}\text{N}_{16-x}\text{O}_{2+x}$  ( $x \approx 2$ )<sup>[16]</sup> (right).

atom is formally inserted into the Si–Si bond, thus leading to two corner-sharing tetrahedrons. The Si–Si distance for these oxygen-linked Si atoms are 310.1(4) pm, the Si–O–Si angle is  $152.3(2)^\circ$ .<sup>[16]</sup> In the meantime we have also obtained  $\text{BaSi}_6\text{N}_8\text{O}$ , which is isotopic with the sialon  $\text{Sr}_2\text{Al}_x\text{Si}_{12-x}\text{N}_{16-x}\text{O}_{2+x}$  ( $x \approx 2$ ).<sup>[17]</sup>

A first validation of the crystal structure of  $\text{SrSi}_6\text{N}_8$  was performed computationally by using standard density functional theory methods (see Experimental Section). After complete geometry optimization of the crystal structure of  $\text{SrSi}_6\text{N}_8$ , we obtained lattice parameters that agree perfectly with the experimental findings. Our results, which were calculated within both the local density approximation (LDA) and the generalized gradient approximation (GGA), reflect the usual trend of these functionals to provide lower and upper boundaries for  $a$ ,  $b$ , and  $c$  within 1% of the experimentally determined values.

We obtained values of 233.3 pm (LDA) and 237.7 pm (GGA) for the Si–Si bond length. These values nicely enclose the experimental value of 235.2(2) pm. The nature of the covalent Si–Si bond was analyzed further by the electron localization function (ELF). The ELF isosurface plot of the central  $\text{N}_3\text{Si–SiN}_3$  fragment within the crystal structure of  $\text{SrSi}_6\text{N}_8$ , accessed at a value of 0.88, is shown in Figure 3. In the center of the Si–Si bond we found a maximum ELF value of

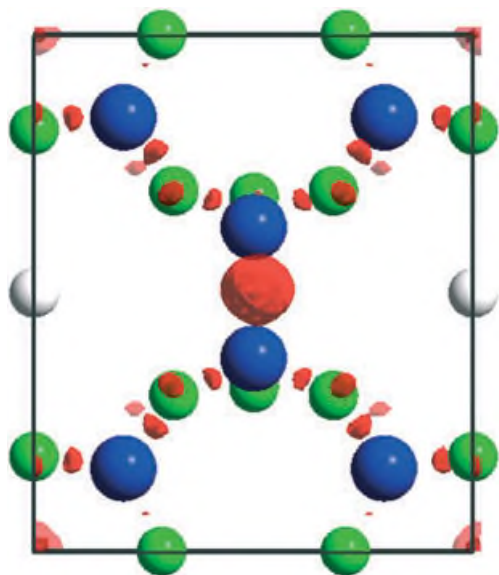


**Figure 3.** ELF of valence electrons in  $\text{SrSi}_6\text{N}_8$  (Sr white, Si blue, and N green), view along  $[00\bar{1}]$ . To enhance the clarity, the figure shows the ELF around the central  $\text{N}_3\text{Si-SiN}_3$  unit only ( $-0.2 \leq z \leq 0.3$ ). The iso-surface is shown for  $\text{ELF} = 0.88$ , which is approximately the maximum of the ELF found within the Si-N bonds. Compared to the view in Figure 2, in this case the unit cell has been translated by the vector  $[\frac{1}{2}00]$ .

nearly 1.0, which indicates an almost ideal pairing of two electrons of opposite spin in a bonding crystal orbital.

One of the strengths of the computational approach is the ability to test the properties of a hypothetical “ $\text{SrSi}_6\text{N}_8\text{O}$ ” by inserting an oxygen atom into the Si-Si bond. After complete optimization of the structure ( $\text{SrSi}_6\text{N}_8\text{O}$ :  $a = 810.3/820.6$ ,  $b = 962.3/972.1$ , and  $c = 480.0/486.5$  pm calculated by LDA/GGA, respectively), we obtained unit cell parameters  $a$  and  $b$ , which differ significantly from the experimentally determined lattice parameters of  $\text{SrSi}_6\text{N}_8$ .<sup>[14]</sup> Insertion of the oxygen atom extends  $b$  by more than 3%, mainly due to the increased spacing between the two Si atoms bound to O. Furthermore, this causes a rotation of the  $\text{SiN}_4$  tetrahedrons of the SiN-framework structure, which becomes visible by comparing the left- and right-hand side of Figures 1 and 2. As a net effect, the cell parameter  $a$  increases by more than 4%. Moreover, although the computed atomic positions of  $\text{SrSi}_6\text{N}_8$  match those obtained from the refinement procedure within 2 pm, atomic positions of the hypothetical oxygen-containing compound  $\text{SrSi}_6\text{N}_8\text{O}$  are shifted by up to 50 pm. The computational results, therefore, corroborate the structure and bonding of the reduced silicate  $\text{SrSi}_6\text{N}_8$ . In particular, they unequivocally establish the single bond between the two Si atoms. However, given the existence of  $\text{BaSi}_6\text{N}_8\text{O}$ ,<sup>[17]</sup> it would appear that it should be possible to find a synthetic pathway to  $\text{SrSi}_6\text{N}_8\text{O}$  as well, for instance by a topotactic diffusion of oxygen into  $\text{SrSi}_6\text{N}_8$ . Conversely, one can envisage transforming  $\text{BaSi}_6\text{N}_8\text{O}$  into  $\text{BaSi}_6\text{N}_8$  topotactically by elimination of oxygen. Currently, we are investigating the compounds  $\text{AESi}_6\text{N}_8(\text{O})$  with  $\text{AE} = \text{Ca}, \text{Sr}, \text{or Ba}$  by both theoretical and experimental methods.

To obtain further proof for the existence of a Si-Si bond in  $\text{SrSi}_6\text{N}_8$ , we conducted  $^{29}\text{Si}$  solid-state NMR investigations. The NMR spectrum in Figure 4 clearly confirms the results from the single-crystal structure analysis. The two  $^{29}\text{Si}$

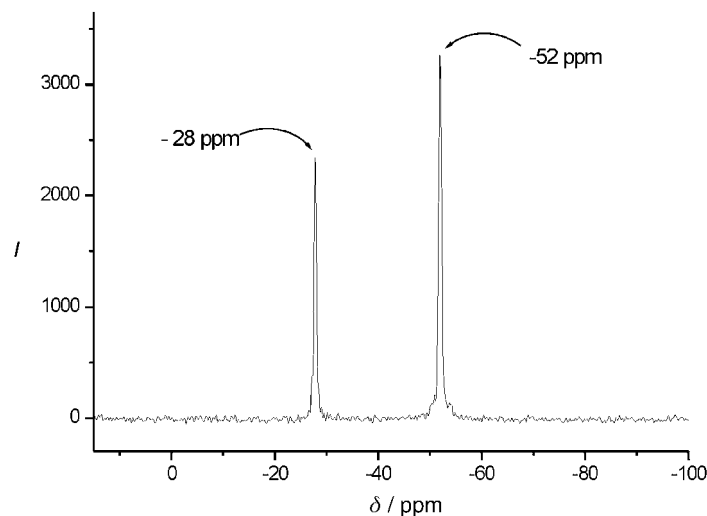


**Figure 4.**  $^{29}\text{Si}$  NMR spectrum of  $\text{SrSi}_6\text{N}_8$ . The two signals derive from  $\text{SiN}_4$  ( $\delta = -52$  ppm) and from  $\text{N}_3\text{Si-SiN}_3$  ( $\delta = -28$  ppm), respectively.

resonances show an intensity ratio of 1:2 corresponding to the multiplicity of the Wyckoff sites  $4d$  ( $(\text{SiN}_3)_2$ ) and  $8e$  ( $\text{SiN}_4$ ). The chemical shift of  $\delta = -52$  ppm is assigned to  $\text{SiN}_4$  tetrahedrons (cf.  $\delta(\text{SiN}_4) = -50$  ppm in  $c\text{-Si}_3\text{N}_4$ <sup>[18]</sup> or  $\delta(\text{SiN}_4) = -64.5/-56.5$  ppm in  $\text{LaSi}_3\text{N}_5$ <sup>[19]</sup>). In contrast, the signal at  $\delta = -28$  ppm corresponds to the  $(\text{SiN}_3)_2$  group. The strong low-field shift could also be caused by carbon-containing  $\text{SiX}_4$  tetrahedrons ( $X = \text{N}, \text{C}$ ), cf.  $\delta(\text{SiC}_4) \approx -20$  ppm in  $\text{SiC}$ <sup>[20]</sup> or  $\delta(\text{SiCN}_3) \approx 37$  ppm in  $\text{Y}_2\text{Si}_4\text{N}_6\text{C}$ .<sup>[21]</sup> However, the presence of carbon has been unequivocally ruled out by chemical analyses. Furthermore, oxygen within the coordination sphere of Si would rather lead to a high-field shift (e.g.  $\delta(\text{SiON}_3) = -61.2$  ppm in  $\text{Si}_2\text{N}_2\text{O}$  (sinoite) or  $\delta(\text{SiO}_2\text{N}_2) = -75.3$  ppm in  $\text{SiON}$  glasses<sup>[22], [23]</sup>).

$\text{SrSi}_6\text{N}_8$  thus represents the first crystalline ternary silicate with a partially reduced silicate substructure in which Si is present in the oxidation states +III and +IV. Recently, another silicate with Si in two oxidation states (+IV and -I) was reported, namely  $\text{Cs}_{10}\text{Si}_7\text{O}_9$ . However, according to the formula  $\text{Cs}_{10}[\text{Si}_4][\text{Si}_3\text{O}_9]$ , this mixed silicide silicate contains isolated  $[\text{Si}_4]^{4-}$  Zintl anions and  $[\text{Si}_3\text{O}_9]^{6-}$  Dreier rings, which are not directly bound to each other.<sup>[24]</sup>

### Experimental Section

In a typical experiment Sr (43.8 mg; dendritic, ABCR GmbH & Co. KG, Karlsruhe, 99.95%) and silicon diimide (156.3 mg; synthesized according to reference [13b]) were placed in a tungsten crucible under argon atmosphere inside a glove box (Unilab, Fa. Mbraun, Garching,  $\text{O}_2 < 1$  ppm,  $\text{H}_2\text{O} < 1$  ppm). Subsequently, the crucible was heated inductively in the reactor of a r.f. furnace<sup>[13b]</sup> under  $\text{N}_2$  atmosphere (dried over silica gel/KOH/molecular sieve (pore width 4 Å)/ $\text{P}_2\text{O}_5$  and activated BTS catalyst) to 1630 °C at a rate of 8.9 °Cmin<sup>-1</sup> and then kept at this temperature for 6.5 h. The reaction product was then

cooled down to 900 °C at a rate of about 1 °C min<sup>-1</sup> and then quenched to room temperature by switching off the furnace. A colorless, coarsely crystalline product was obtained, which according to the X-ray powder pattern is single-phase SrSi<sub>6</sub>N<sub>8</sub>. Elemental analysis (double determinations by the Mikroanalytisches Labor Pascher, Remagen) calcd for SrSi<sub>6</sub>N<sub>8</sub> (368.24): Sr 23.8, Si 45.8, N 30.4, O 0.0; found: Sr 23.1, Si 45.9, N 30.7, O < 1.0. The single crystals obtained were suitable for X-ray structure analysis. A theoretical powder diffraction pattern calculated on the basis of the single-crystal data showed excellent agreement with a measured powder diffraction pattern for SrSi<sub>6</sub>N<sub>8</sub> with respect to the positions and intensities of all the observed reflections.

**Calculations:** For density functional<sup>[25]</sup> calculations, we applied the VASP software package.<sup>[26]</sup> The pseudopotentials employed are based on the projector-augmented-wave (PAW) method.<sup>[27]</sup> We used both the local density approximation (LDA) and the generalized-gradient approximation (GGA) to treat the exchange-correlation energy of the electrons. All the results rely on well-converged calculations with respect to cut-off energy (500 eV) and *k*-point sampling (2 × 2 × 4 mesh). Residual forces and stresses in the optimized structures are less than 0.005 eV Å<sup>-1</sup> and 1 kbar, respectively. The electron localization function (ELF) is a local descriptor of the probability of electron pairing.<sup>[28]</sup> By definition the ELF takes values within the interval [-1,1]. ELF tends to zero in regions of space, where the average distances between spin-like and spin-unlike electrons are similar, hence, electrons are unpaired. When spin-unlike electrons are paired, ELF tends to +1; when spin-like electrons are paired, ELF tends to -1. Regions corresponding to electron pairing exhibit a maximum, and all the regions corresponding to a lack of electron pairing exhibit a minimum. Since we are interested in the bonding between the two Si atoms, we focussed on pairing maxima.

- [1] K. Keil, C. A. Andersen, *Nature* **1965**, 207, 745.  
 [2] W. R. Ryall, A. Muan, *Science* **1969**, 165, 1363.  
 [3] a) F. Liebau, *Structural Chemistry of Silicates*, Springer, Berlin, **1985**; b) H. Huppertz, W. Schnick, *Chem. Eur. J.* **1997**, 3, 679.  
 [4] In silicates, higher coordination numbers of Si (CN > 4) are found only in a few cases, mostly high-pressure phases,<sup>[3,5,6]</sup> for example, rutile-type SiO<sub>2</sub> (high-pressure polymorph stishovite), perovskite-type (Mg,Fe)SiO<sub>3</sub> occurring in the deeper mantle of the earth, or hollandite-analogous CaAl<sub>2</sub>Si<sub>2</sub>O<sub>8</sub>.<sup>[5]</sup> At lower pressures a few silicates can be obtained that contain both SiO<sub>6</sub> octahedrons and SiO<sub>4</sub> tetrahedrons (e.g. K<sub>2</sub>Si<sub>4</sub>O<sub>9</sub>,<sup>[7]</sup> BaSi<sub>4</sub>O<sub>9</sub>,<sup>[8]</sup> and Na<sub>1.8</sub>Ca<sub>1.1</sub>Si<sub>6</sub>O<sub>14</sub>.<sup>[9]</sup>).  
 [5] L. W. Finger, R. M. Hazen, *Acta Crystallogr. Sect. B* **1991**, 47, 561.  
 [6] R. M. Hazen, R. T. Downs, L. W. Finger, *Science* **1996**, 272, 1769.  
 [7] D. K. Swanson, C. T. Prewitt, *Am. Mineral.* **1983**, 68, 581.  
 [8] L. W. Finger, R. M. Hazen, B. A. Fursenko, *J. Phys. Chem. Solids* **1995**, 56, 1389.  
 [9] T. Gasparik, J. B. Parise, B. A. Eiben, J. A. Hriljac, *Am. Mineral.* **1995**, 80, 1269.  
 [10] E. Hengge, *Z. Anorg. Allg. Chem.* **1962**, 315, 298.  
 [11] a) R. Kniep, J. Haberecht, PCT Int. Appl. WO 02/096799A2, **2002**; b) J. Haberecht, PhD Thesis, TU Dresden, **2001**.  
 [12] R. M. Hagenmeyer, B. Friede, M. Jansen, *J. Non-Cryst. Solids* **1998**, 226, 225.  
 [13] a) R. Lauterbach, W. Schnick, *Z. Anorg. Allg. Chem.* **1998**, 624, 1154; b) W. Schnick, H. Huppertz, R. Lauterbach, *J. Mater. Chem.* **1999**, 9, 289; c) K. Köllisch, W. Schnick, *Angew. Chem.* **1999**, 111, 368; *Angew. Chem. Int. Ed.* **1999**, 38, 357; d) R. Lauterbach, W. Schnick, *Z. Anorg. Allg. Chem.* **2000**, 626, 56; e) E. Irran, K. Köllisch, S. Leoni, R. Nesper, P. F. Henry, M. T. Weller, W. Schnick, *Chem. Eur. J.* **2000**, 6, 2714; f) R. Lauterbach, E. Irran, P. F. Henry, M. T. Weller, W. Schnick, *J. Mater. Chem.* **2000**, 10, 1357; g) R. Lauterbach, W. Schnick, *Solid State Sci.* **2000**, 2, 463; h) H. A. Höpfe, G. Kotzba, R. Pöttgen, W. Schnick, *J. Solid State Chem.* **2002**, 167, 393.  
 [14] Crystal structure data of SrSi<sub>6</sub>N<sub>8</sub>: STOIE IPDS, Mo<sub>Kα</sub> (71.073 pm), 2θ<sub>max</sub> = 65°, crystal size 0.11 × 0.09 × 0.04 mm<sup>3</sup>, orthorhombic, space group *Imm2* (no. 44), *a* = 785.5(2), *b* = 925.9(2), *c* = 480.1(1) pm, *V* = 0.3492(2) nm<sup>3</sup>, *Z* = 2, ρ<sub>calcd</sub> = 3.507 g cm<sup>-3</sup>, μ<sub>MoKα</sub> = 8.717 mm<sup>-1</sup>, 2242 measured reflections, 694 of which are independent, *R*<sub>int</sub> = 0.030, least-squares refinement (all atoms anisotropic) on *F*<sup>2</sup> (G. M. Sheldrick, SHELXL-97, program for the refinement of crystal structures, Universität Göttingen, Göttingen (Deutschland), **1997**); semiempirical absorption correction (min./max. transmission factor 0.249/0.292), Flack parameter η = 0.565(9), refined as an inversion twin, *R* values (all data/*F*<sub>o</sub><sup>2</sup> ≥ 2σ(*F*<sub>o</sub><sup>2</sup>)) *R*<sub>1</sub> = 0.0239/0.0218, *wR*<sub>2</sub> = 0.0487/0.0482, GooF = 0.978 for 657 observed reflections (*F*<sub>o</sub><sup>2</sup> ≥ 2σ(*F*<sub>o</sub><sup>2</sup>)) and 43 refined parameters. Further details on the crystal structure investigations may be obtained from the Fachinformationszentrum Karlsruhe, 76344 Eggenstein-Leopoldshafen, Germany (fax: (+49)7247-808-666; e-mail: crysdata@fiz-karlsruhe.de), on quoting the depository number CSD-391265.  
 [15] S. G. Cho, O. K. Rim, G. Park, *J. Comput. Chem.* **1997**, 18, 1523.  
 [16] Z. Shen, J. Grins, S. Esmailzadeh, H. Ehrenberg, *J. Mater. Chem.* **1999**, 9, 1019.  
 [17] Crystal data of BaSi<sub>6</sub>N<sub>8</sub>O: space group *Imm2* (no. 44), *a* = 808.5(2), *b* = 967.2(2), *c* = 483.4(1) pm, *V* = 0.378 nm<sup>3</sup>, *Z* = 2, F. Stadler, S. Schmid, W. Schnick, unpublished results.  
 [18] T. Sekine, M. Tansho, M. Kanzaki, *Appl. Phys. Lett.* **2001**, 78, 3050.  
 [19] G. R. Hatfield, B. Li, W. B. Hammond, F. Reidinger, J. Yamanis, *J. Mater. Sci.* **1990**, 25, 4032.  
 [20] J. S. Hartman, M. F. Richardson, B. L. Sherriff, B. G. Winsborrow, *J. Am. Chem. Soc.* **1987**, 109, 6059.  
 [21] S. Schmolke, J. Senker, W. Schnick, unpublished results.  
 [22] S. Kohn, W. Hoffbauer, M. Jansen, R. Franke, S. Bender, *J. Non-Cryst. Solids* **1998**, 224, 232.  
 [23] Double-quantum <sup>29</sup>Si solid-state NMR experiments with <sup>29</sup>Si-enriched samples (natural abundance of <sup>29</sup>Si is only 4.70 %) confirm the obtained results: F. Stadler, J. Senker, W. Schnick, unpublished results.  
 [24] S. Hoffmann, T. F. Fässler, C. Hoch, C. Röhr, *Angew. Chem.* **2001**, 113, 4527; *Angew. Chem. Int. Ed.* **2001**, 40, 4398.  
 [25] P. Hohenberg, W. Kohn, *Phys. Rev. A* **1964**, 136, 864.  
 [26] a) G. Kresse, J. Hafner, *Phys. Rev. B* **1993**, 47, 558; b) G. Kresse, J. Hafner, *Phys. Rev. B* **1994**, 49, 14251; c) G. Kresse, J. Furthmüller, *Comput. Mater. Sci.* **1996**, 6, 15; d) G. Kresse, J. Furthmüller, *Phys. Rev. B* **1996**, 54, 11169.  
 [27] a) P. E. Blöchl, *Phys. Rev. B* **1994**, 50, 7953; b) G. Kresse, D. Joubert, *Phys. Rev. B* **1999**, 59, 1758.  
 [28] a) A. D. Becke, K. E. Edgcombe, *J. Chem. Phys.* **1990**, 92, 5397; b) A. Savin, A. D. Becke, J. Flad, R. Nesper, H. Preuß, H. G. von Schnering, *Angew. Chem.* **1991**, 103, 421; *Angew. Chem. Int. Ed. Engl.* **1991**, 30, 409.